Chapter 2

Power Flow Algorithms for Ill-conditioned Unbalanced Distribution Systems

2.1 Introduction

Most of the power systems are well-conditioned and their PF problem can be easily evaluated using NR-based algorithms. Nevertheless, in certain circumstances, the conditions of the system may become ill-conditioned. Consequently, the aforementioned algorithms can diverge or have poor convergence characteristics. This chapter addresses the issue of solving PF for ill-conditioned distribution system and proposes some numerical techniques to solve these kind of problems.

For the steady-state analysis, solving the PF problem has been one of the major area of investigation in the power systems since mid 1950s [111]. Different methods have been proposed to solve the PF problem in the literature. Different metrics are utilized to compare these algorithms on the basis of basic requirements of PF calculations. These metrics are as follows: (i) The memory requirements and CPU time (computing efficiency). (ii) The reliability and flexibility of algorithms. (iii) The convergence characteristics of algorithms.

In a power system, determining the voltage magnitude and phase of each bus, as well as the flow of active and reactive power through each bus, are the main objectives of the PF problem. In some circumstances, the Jacobian matrix may get near singular or may

become singular during the evaluation process when using NR-like algorithms [59]. When the Jacobian matrix is non-singular during the evaluation of solutions, the PF solution can be obtained using a flat initial start. This system is said to be well-conditioned and PF solution can be easily evaluated using conventional NR-based algorithms within a small number of iterations [59]. In some cases, the PF solution of the system exists, but conventional NR-based algorithms cannot provide the solution due to the near-singularity or singularity of the Jacobian matrix. In this situation, the power system is termed as ill-conditioned or bad-conditioned [112, 113]. In ill-conditioned power systems, the PF solution is very sensitive to small variations of the elements of the Jacobian matrix [70,114]. There are several reasons which may lead to deterioration of the condition of the system to ill-condition such as, high ratio of r/x, installation of some types of equipment, and location of the swing bus, etc. To solve the PF problem, one of the most popular numerical methods is the NR algorithm. Some of the popular algorithms are second-order NR-based algorithms which are utilized to solve ill-conditioned test systems. In [115], a fast-decoupled version was proposed to solve the PF problem of systems with high r/x ratio lines. In [57], a second-order PF algorithm has been proposed to deal with PF problem of distribution systems. Iwamoto *et.al.* propose a most popular NR-based algorithm for ill-conditioned PF solution [60]. In literature, several algorithms have been proposed to address the PF problem of ill-conditioned power systems [10, 61–66]. In [69], the LM algorithm has been proposed to solve the PF problem in ill-conditioned systems. In [70], a CN method is developed to solve the PF problem in ill-conditioned systems. Additionally, several algorithms based on LM and CN have been proposed in [71, 72]. Authors of [73] have presented a variant of LM to solve the PF problem in case of ill-conditioned as well as well-conditioned power systems. Authors of [70] have proposed a RK4 algorithm to solve the PF problem. To solve the PF problem, high-order NR-based algorithms have been proposed in [59].

The above-mentioned works have been studied on the transmission system which is ill-conditioned due to high loading conditions. However, in the distribution system, some features that are distinct from the transmission system make the system ill-conditioned [15]. There features are (i) weakly meshed or radial topology, (ii) having high r/x ratio, and (iii) having unbalanced system load. To address these issues, topology based algorithms have been proposed but these algorithms are only applicable to single source

systems.

Due to the increase of penetration of DGs in the distribution systems, many algorithms have been proposed to solve the PF problem of distribution system having DGs. Authors of [116,117] have proposed different models of various equipment of distribution system (i.e. DGs and voltage regulators) to solve the distribution PF problem. In these approaches, DGs can be modeled as PV bus or as PQ bus. In [118], three different mathematical models of DGs have been proposed and these models are (1) constant voltage model, (2) variable reactive power model, and (3) constant power factor model.

Earlier, the PV buses were rare in the distribution system, but in the modern distribution systems, substantial number of PV buses can be present. Regular PF routines based on NR have limitations of convergence when applied to distribution systems due to large number of PV buses which makes the system ill-conditioned. The development of backward/forward sweep method mitigated this problem of convergence. However, forward/backward methods have limitations in handling PV buses.

In this chapter, simplified, generalized and efficient algorithms are proposed to solve the PF problem of the ill-conditioned unbalanced three-phase distribution system. Different models of DGs are also incorporated in this algorithms. These algorithms are based on LM and CN which are simple because these approaches depend mainly on the Jacobian matrix similar to NR-based algorithms. A strategy to control the step-size or the acceleration factor of LM and CN has been proposed to avoid ill-conditioning of the Jacobian. Further the problem of determining the step-size has been considered as an optimization sub-problem within the framework of CN and LM algorithm. The proposed modifications provide good convergence rate in different operating conditions. Moreover, they are generalized because they incorporate more accurate load modeling, unbalanced loads, three-phase modeling of feeders and different DG modeling. These algorithms are benchmarked on several unbalanced radial distribution systems (some of them are available in [119]). Different case studies have been performed to demonstrate the robustness and efficiency of these algorithms.

The outline of this chapter is as follows. In Section 2.2, PF formulations based on current injection and power injection are discussed with the calculation procedure of the Jacobian matrix. Section 2.3 presents the procedure of proposed algorithms for solving the PF problems. In Section 2.4, different numerical examples are performed to demonstrate

the robustness and validity of the proposed algorithm on different operating cases.

2.2 Problem Formulation

In this section, the PF formulation based on power injection and current injection is briefly discussed. Moreover, the calculation procedure of the Jacobian matrix is also included.

2.2.1 Formulation based on Power Injection

The PF problem can be represented by the power balance equation at each bus. Reactive and active powers are specified at each PQ buses (load buses) and only active power is specified at PV buses (generator buses). These active and reactive power can also be calculated using bus voltages and system Admittance Matrix (Ybus), which are termed as calculated power. The solution to PF problem is bus voltages (magnitude and phase angle) where the difference of specified power and calculated power at each bus become zero or within the specified tolerance limit. Consequently, the main objective of PF is to calculate the voltage magnitude and angles of the system buses that equals the specified power and the calculated power at each bus of the system. Hence, the PF problem can be treated as a system of non-linear equations.

In polar co-ordinates, the power balance equation at k-th bus can be represented by the following equations.

$$P_k - \sum_{i=1}^{N} |V_k||V_i||Y_{ki}|cos(\delta_k - \delta_i - \theta_{ki}) = 0, \tag{2.1}$$

$$Q_k - \sum_{i=1}^{N} |V_k||V_i||Y_{ki}|sin(\delta_k - \delta_i - \theta_{ki}) = 0, \tag{2.2}$$

where $P_k(= P_{g,k} - P_{l,k})$ and $Q_k(= Q_{g,k} - Q_{l,k})$ are total active and reactive power injected at the k-th bus, respectively, $V_k(|V_k|\angle\delta_k)$ represents the bus voltage at the k-th bus, and $Y_{ki}(|Y_{ki}|\angle\theta_{ki})$ represents the ij-th element of admittance matrix. Here, $P_{g,k}$ and $Q_{g,k}$ are total generated active and reactive power at the k-th bus, respectively, $P_{l,k}$ and $Q_{l,k}$ represent total required active and reactive load at the k-th bus.

Formation of Jacobian matrix:

To derive the elements of the Jacobian matrix,

$$P_k - \sum_{i=1}^{N} |V_k||V_i||Y_{ki}|cos(\delta_k - \delta_i - \theta_{ki}) = P_k - |V_k|^2 G_{kk} - \sum_{i=1,i\neq k}^{N} |V_k||V_i||Y_{ki}|cos(\delta_k - \delta_i - \theta_{ki}) = 0,$$
(2.3)

$$Q_k - \sum_{i=1}^{N} |V_k||V_i||Y_{ki}|sin(\delta_k - \delta_i - \theta_{ki}) = Q_k - |V_k|^2 B_{kk} - \sum_{i=1,i\neq k}^{N} |V_k||V_i||Y_{ki}|sin(\delta_k - \delta_i - \theta_{ki}) = 0,$$
(2.4)

where $G_{kk} = |Y_{kk}|cos(\theta_{kk})$ and $B_{kk} = |Y_{kk}|sin(\theta_{kk})$.

The elements of Jacobian matrix can be calculated as follows.

$$\frac{\partial P_i}{\partial \delta_j} = - \sum_{k=1,k\neq i}^{N} |V_i||V_k||Y_{ik}|sin(\delta_i - \delta_k - \theta_{ik}); j = i,$$
(2.5)

$$\frac{\partial P_i}{\partial \delta_j} = |V_i||V_j||Y_{ij}|sin(\delta_i - \delta_j - \theta_{ij}); j \neq i,$$
(2.6)

$$\frac{\partial P_i}{\partial |V_j|} = 2|V_i|G_{ii} + \sum_{k=1,k\neq i}^{N} |V_k||Y_{ik}|cos(\delta_i - \delta_k - \theta_{ik}); j = i,$$
(2.7)

$$\frac{\partial P_i}{\partial |V_i|} = |V_i||Y_{ij}|cos(\delta_i - \delta_j - \theta_{ij}); j \neq i,$$
(2.8)

$$\frac{\partial Q_i}{\partial \delta_j} = \sum_{k=1,k\neq i}^{N} |V_i||V_k||Y_{ik}|cos(\delta_i - \delta_k - \theta_{ik}); j = i,$$
(2.9)

$$\frac{\partial Q_i}{\partial \delta_j} = -2V_i B_{ii} + \sum_{k=1,k\neq i}^{N} |V_k||Y_{ik}|sin(\delta_i - \delta_k - \theta_{ik}); j = i, \text{and}$$
(2.10)

$$\frac{\partial Q_i}{\partial |V_j|} = |V_i||Y_{ij}|sin(\delta_i - \delta_j - \theta_{ij}); j \neq i$$
(2.11)

Taylor's expansion of Equations 2.3 and 2.4 can be written as follows in compact form.

$$\begin{bmatrix} \frac{\partial P_2}{\partial \delta_2} & :: & \frac{\partial P_2}{\partial \delta_N} & \frac{\partial P_2}{V_2} & :: & \frac{\partial P_2}{\partial V_N} \\ :: & :: & :: & :: & :: & :: \\ \frac{\partial P_N}{\partial \delta_2} & :: & \frac{\partial P_N}{\partial \delta_N} & \frac{\partial P_N}{V_2} & :: & \frac{\partial P_N}{\partial V_N} \\ \frac{\partial Q_2}{\partial \delta_2} & :: & \frac{\partial Q_2}{\partial \delta_N} & \frac{\partial Q_2}{V_2} & :: & \frac{\partial Q_2}{\partial V_N} \\ :: & :: & :: & :: & :: & :: \\ \frac{\partial Q_N}{\partial \delta_2} & :: & \frac{\partial Q_N}{\partial \delta_N} & \frac{\partial Q_N}{V_2} & :: & \frac{\partial Q_N}{\partial V_N} \end{bmatrix} \begin{bmatrix} \triangle\delta_2 \\ :: \\ \triangle\delta_N \\ \triangle V_2 \\ :: \\ \triangle V_N \end{bmatrix} = \begin{bmatrix} P_2^{sp} - P_2(\boldsymbol{\delta}^{(0)}, \boldsymbol{V}^{(0)}) \\ :: \\ P_N^{sp} - P_N(\boldsymbol{\delta}^{(0)}, \boldsymbol{V}^{(0)}) \\ Q_2^{sp} - Q_2(\boldsymbol{\delta}^{(0)}, \boldsymbol{V}^{(0)}) \\ :: \\ Q_N^{sp} - Q_N(\boldsymbol{\delta}^{(0)}, \boldsymbol{V}^{(0)}) \end{bmatrix}$$
(2.12)

where $P_i(\boldsymbol{\delta}^{(0)}, \boldsymbol{V}^{(0)})$ and $Q_i(\boldsymbol{\delta}^{(0)}, \boldsymbol{V}^{(0)})$ are the calculated injected active and reactive power, respectively, at i-th bus. With new notation, the Equation 2.12 can be written as

$$\begin{bmatrix} \boldsymbol{J1} & \boldsymbol{J2} \\ \boldsymbol{J3} & \boldsymbol{J4} \end{bmatrix} \begin{bmatrix} \triangle\boldsymbol{\delta} \\ \triangle\boldsymbol{V} \end{bmatrix} = \begin{bmatrix} \triangle\boldsymbol{P} \\ \triangle\boldsymbol{Q} \end{bmatrix} \tag{2.13}$$

where,

$$\boldsymbol{J1} = \frac{\partial \boldsymbol{P}}{\partial \boldsymbol{\delta}} = \begin{bmatrix} \frac{\partial P_2}{\partial \delta_2} & :: & \frac{\partial P_2}{\partial \delta_N} \\ :: & :: & :: \\ \frac{\partial P_N}{\partial \delta_2} & :: & \frac{\partial P_N}{\partial \delta_N} \end{bmatrix}, \tag{2.14}$$

$$\boldsymbol{J2} = \frac{\partial \boldsymbol{P}}{\partial \boldsymbol{V}} = \begin{bmatrix} \frac{\partial P_2}{\partial V_2} & :: & \frac{\partial P_2}{\partial V_N} \\ :: & :: & :: \\ \frac{\partial P_N}{\partial V_2} & :: & \frac{\partial P_N}{\partial V_N} \end{bmatrix}, \tag{2.15}$$

$$\boldsymbol{J3} = \frac{\partial \boldsymbol{Q}}{\partial \boldsymbol{\delta}} = \begin{bmatrix} \frac{\partial Q_2}{\partial \delta_2} & :: & \frac{\partial Q_2}{\partial \delta_N} \\ :: & :: & :: \\ \frac{\partial Q_N}{\partial \delta_2} & :: & \frac{\partial Q_N}{\partial \delta_N} \end{bmatrix}, \text{ and} \tag{2.16}$$

$$\boldsymbol{J4} = \frac{\partial \boldsymbol{Q}}{\partial \boldsymbol{V}} = \begin{bmatrix} \frac{\partial Q_2}{\partial V_2} & :: & \frac{\partial Q_2}{\partial V_N} \\ :: & :: & :: \\ \frac{\partial Q_N}{\partial V_2} & :: & \frac{\partial Q_N}{\partial V_N} \end{bmatrix}. \tag{2.17}$$

Equation 2.13 creates a basis for the NR-based algorithms. In this work, two power injection based algorithm are proposed which utilize the Jacobian matrix (explained in Equation 2.13) for updating the solution.

2.2.2 Formulation based on Current Injection

Power injection based PF formulation has been dealth in the above section. In this subsection, the current injection based PF formulation for power systems is proposed which is more accurate than the conventional power injection based formulation. Conventional power injection based formulation does not account for the voltage dependency of the loads which should not be ignored in distribution systems. The PF equation are expressed in rectangular coordinates i.e, elements of nodal admittance matrix, bus voltages, injected powers, and current injections are represented in rectangular coordinates.

The active and reactive current mismatch, for a given bus k, is given by the following relation.

$$\Delta I_{rk} = \sum_{i=1}^{n}(G_{ki}V_{ri} - B_{ki}V_{mi}) - \frac{P_k V_{rk} + Q_k V_{mk}}{(V_{rk})^2 + (V_{mk})^2}, \tag{2.18}$$

$$\Delta I_{mk} = \sum_{i=1}^{n}(B_{ki}V_{ri} + G_{ki}V_{mi}) - \frac{P_k V_{mk} - Q_k V_{rk}}{(V_{rk})^2 + (V_{mk})^2}. \tag{2.19}$$

Total injected active and reactive powers can be calculated by following equations.

$$P_k = P_{g,k} - P_{l,k}, \tag{2.20}$$

$$Q_k = Q_{g,k} - Q_{l,k}. \tag{2.21}$$

The voltage dependency of loads are represented by the following polynomial equations.

$$P_{lk} = P_{0k}\{\alpha_p + \beta_p V_k + \gamma_p V_k{}^2\}, \tag{2.22}$$

$$Q_{lk} = Q_{0k}\{\alpha_q + \beta_q V_k + \gamma_q V_k{}^2\}. \tag{2.23}$$

Where,

$$\alpha_p + \beta_p + \gamma_p = 1$$

and,

$$V_k = (V_{rk}^2 + V_{mk}^2)^{\frac{1}{2}}.$$

Similarly,

$$\alpha_q + \beta_q + \gamma_q = 1.$$

Taylor's series expansion of equations (2.18) and (2.19) after neglecting the higher order terms, gives the following equations.

$$\begin{bmatrix} \Delta I_{rk} \\ \Delta I_{mk} \end{bmatrix} = \sum_{\substack{i=1, \\ i \neq k}}^{n} \begin{bmatrix} G_{ki} & -B_{ki} \\ B_{ki} & G_{ki} \end{bmatrix} \begin{bmatrix} \Delta V_{ri} \\ \Delta V_{mi} \end{bmatrix}$$
$$+ \begin{bmatrix} G'_{kk} & B'_{kk} \\ B''_{kk} & G''_{kk} \end{bmatrix} \begin{bmatrix} \Delta V_{rk} \\ \Delta V_{mk} \end{bmatrix} \tag{2.24}$$
$$- \frac{1}{V_k^2} \begin{bmatrix} V_{rk} & V_{mk} \\ V_{mk} & -V_{rk} \end{bmatrix} \begin{bmatrix} \Delta P_k \\ \Delta Q_k \end{bmatrix}.$$

Where, the values of G'_{kk}, B'_{kk}, G''_{kk} and B''_{kk} depend on the type of kth bus (PQ/PV).

Representation of PQ buses:

In case of PQ buses, injected real and reactive powers are specified on the buses, i.e. $P_k = P_k^{sp}$ and $Q_k = Q_k^{sp}$, where 'k' is the PQ bus.

G_{kk}', B_{kk}', G_{kk}'' and B_{kk}'' can be expressed as follows.

$$G_{kk}' = G_{kk} - \frac{1}{V_k^4}\{(V_{mk}^2 - V_{rk}^2)P_k^{sp} - 2V_{mk}V_{rk}Q_k^{sp}\}, \qquad (2.25)$$

$$B_{kk}' = -B_{kk} - \frac{1}{V_k^4}\{(V_{rk}^2 - V_{mk}^2)Q_k^{sp} - 2V_{mk}V_{rk}P_k^{sp}\}, \qquad (2.26)$$

$$B_{kk}'' = B_{kk} - \frac{1}{V_k^4}\{(V_{rk}^2 - V_{mk}^2)Q_k^{sp} - 2V_{mk}V_{rk}P_k^{sp}\}, \qquad (2.27)$$

$$G_{kk}'' = G_{kk} + \frac{1}{V_k^4}\{(V_{mk}^2 - V_{rk}^2)P_k^{sp} - 2V_{mk}V_{rk}Q_k^{sp}\}. \qquad (2.28)$$

Where,

$$P_k^{sp} = P_g - P_{0k}\{\alpha_p + \beta_p V_k + \gamma_p V_k^2\},$$

$$Q_k^{sp} = Q_g - Q_{0k}\{\alpha_q + \beta_q V_k + \gamma_q V_k^2\}.$$

The values of ΔP_k and ΔQ_k are calculated as follows.

$$\Delta P_k = \Delta P_g - P_{0k}\beta_p\Delta V_k - 2V_k\gamma_p\Delta V_k. \qquad (2.29)$$

Similarly,

$$\Delta Q_k = \Delta Q_g - Q_{0k}\beta_q\Delta V_k - 2V_k\gamma_q\Delta V_k. \qquad (2.30)$$

Substituting $\Delta P_g = 0$ and $\Delta Q_g = 0$ at PQ buses,

$$\Delta P_k = -P_{0k}\left(\beta_p + 2V_k\gamma_p\right)\Delta V_k,$$

$$\Delta Q_k = -Q_{0k}\left(\beta_q + 2V_k\gamma_q\right)\Delta V_k$$

and,

$$\Delta V_k = \frac{1}{V_k}\left(V_{rk}\Delta V_{rk} + V_{mk}\Delta V_{mk}\right). \qquad (2.31)$$

This yields,

$$\Delta P_k = -\frac{P_{ok}}{V_k}\left(\beta_p + 2V_k\gamma_p\right)\left(V_{rk}\Delta V_{rk} + V_{mk}\Delta V_{mk}\right),$$

$$\Delta Q_k = -\frac{Q_{ok}}{V_k}\left(\beta_q + 2V_k\gamma_q\right)\left(V_{rk}\Delta V_{rk} + V_{mk}\Delta V_{mk}\right).$$

Substituting the expressions of ΔP_k and ΔQ_k in equation (2.24), yields,

$$\begin{bmatrix} \Delta I_{rk} \\ \Delta I_{mk} \end{bmatrix} = \sum_{\substack{i=1, \\ i\neq k}}^{n} \begin{bmatrix} G_{ki} & -B_{ki} \\ B_{ki} & G_{ki} \end{bmatrix} \begin{bmatrix} \Delta V_{ri} \\ \Delta V_{mi} \end{bmatrix}$$
$$+ \begin{bmatrix} G'_{kk} & B'_{kk} \\ B''_{kk} & G''_{kk} \end{bmatrix} \begin{bmatrix} \Delta V_{rk} \\ \Delta V_{mk} \end{bmatrix} \tag{2.32}$$
$$- \begin{bmatrix} A & B \\ C & D \end{bmatrix} \begin{bmatrix} \Delta V_{rk} \\ \Delta V_{mk} \end{bmatrix}.$$

Where,

$$A = \frac{-P_{0k}V_{rk}^2\,(\beta_p + 2\gamma_p V_k) - Q_{0k}V_{rk}V_{mk}\,(\beta_q + 2\gamma_q V_k)}{V_k^3},$$

$$B = \frac{-P_{0k}V_{rk}V_{mk}\,(\beta_p + 2\gamma_p V_k) - Q_{0k}V_{mk}^2\,(\beta_q + 2\gamma_q V_k)}{V_k^3},$$

$$C = \frac{-P_{0k}V_{rk}V_{mk}\,(\beta_p + 2\gamma_p V_k) + Q_{0k}V_{rk}^2\,(\beta_q + 2\gamma_q V_k)}{V_k^3},$$

$$D = \frac{-P_{0k}V_{mk}^2\,(\beta_p + 2\gamma_p V_k) + Q_{0k}V_{rk}V_{mk}\,(\beta_q + 2\gamma_q V_k)}{V_k^3}.$$

Representation of PV bus:

In case of PV bus 'k', Q_k is not specified. For a PV bus, Q_k is calculated in every iteration by using the following equation.

$$Q_k = V_{mk}I_{rk}^{cal} - V_{rk}I_{mk}^{cal}. \tag{2.33}$$

Substituting the values of Q_k in equation (2.25), (2.26), (2.27) and (2.28) following expressions of G'_{kk}, B'_{kk}, G''_{kk} and B''_{kk} are obtained.

$$G'_{kk} = G_{kk} - \frac{1}{V_k^4}(V_{mk}^2\{P_k^{sp} - 2V_{rk}I_{rk}^{cal}\} - V_{rk}^2\{P_k^{sp} + 2V_{mk}I_{mk}^{cal}\}), \tag{2.34}$$

$$B'_{kk} = -B_{kk} - \frac{1}{V_k^4}(V_{mk}\{(V_{rk}^2 - V_{mk}^2)I_{rk}^{cal} - V_{rk}P_k^{sp}\} - V_{rk}\{(V_{rk}^2 - V_{mk}^2)I_{mk}^{cal} - V_{mk}P_k^{sp}\}), \tag{2.35}$$

$$B''_{kk} = B_{kk} - \frac{1}{V_k^4}(V_{mk}\{(V_{rk}^2 - V_{mk}^2)I_{rk}^{cal} - V_{rk}P_k^{sp}\} - V_{rk}\{(V_{rk}^2 - V_{mk}^2)I_{mk}^{cal} - V_{mk}P_k^{sp}\}), \tag{2.36}$$

$$G_{kk}^{''} = G_{kk} + \frac{1}{V_k^4}(V_{mk}^2(P_k^{sp} - 2V_{rk}I_{rk}^{cal}) - V_{rk}^2(P_k^{sp} + 2V_{mk}I_{mk}^{cal})). \tag{2.37}$$

Since, for a PV bus, ΔP_g and $\Delta V_k = 0$, equations (2.29) and (7.18) get reduced as follows,

$$\Delta P_k = \Delta P_g = 0,$$

$$\Delta Q_k = \Delta Q_{gk}.$$

Substituting $\Delta V_k = 0$ in equation (2.31) yields,

$$\Delta V_{rk} = -\frac{V_{mk}}{V_{rk}}\Delta V_{mk}.$$

Substituting expressions of ΔQ_k and ΔV_{rk} in equation (2.24) yields following expressions.

$$\begin{bmatrix} \Delta I_{rk} \\ \Delta I_{mk} \end{bmatrix} = \sum_{\substack{i=1, \\ i \neq k}}^{n} \begin{bmatrix} G_{ki} & -B_{ki} \\ B_{ki} & G_{ki} \end{bmatrix} \begin{bmatrix} \Delta V_{ri} \\ \Delta V_{mi} \end{bmatrix}$$
$$+ \begin{bmatrix} G_{kk}' & B_{kk}' \\ G_{kk}^{''} & B_{kk}^{''} \end{bmatrix} \begin{bmatrix} -\frac{V_{mk}}{V_{rk}}\Delta V_{mk} \\ \Delta V_{mk} \end{bmatrix} \tag{2.38}$$
$$- \frac{1}{V_k^2} \begin{bmatrix} V_{rk} & V_{mk} \\ V_{mk} & -V_{rk} \end{bmatrix} \begin{bmatrix} 0 \\ \Delta Q_g \end{bmatrix}.$$

Simplification of equation (2.38) yields,

$$\begin{bmatrix} \Delta I_{rk} \\ \Delta I_{mk} \end{bmatrix} = \sum_{\substack{i=1, \\ i \neq k}}^{n} \begin{bmatrix} G_{ki} & -B_{ki} \\ B_{ki} & G_{ki} \end{bmatrix} \begin{bmatrix} \Delta V_{ri} \\ \Delta V_{mi} \end{bmatrix} + \begin{bmatrix} B_{kk}' - \frac{V_{mk}}{V_{rk}}G_{kk}' & -\frac{V_{mk}}{V_k^2} \\ G_{kk}^{''} - \frac{V_{mk}}{V_{rk}}B_{kk}^{''} & \frac{V_{rk}}{V_k^2} \end{bmatrix}$$
$$\begin{bmatrix} \Delta V_{mk} \\ \Delta Q_g \end{bmatrix}. \tag{2.39}$$

After simplifying the equation (2.39), expressions for B_{kk}', G_{kk}', B_{kk}'', and G_{kk}''' becomes as follows.

$$B_{kk}' = -B_{kk} - \frac{V_{mk}I_{rk}^{calc} - V_{rk}I_{mk}^{calc}}{V_k^2}, \tag{2.40}$$

$$G_{kk}' = G_{kk} - \frac{P_k^{sp}}{V_k^2}, \tag{2.41}$$

$$G_{kk}'' = G_{kk} + \frac{P_k^{sp}}{V_k^2}, \tag{2.42}$$

$$B_{kk}'' = B_{kk} - \frac{V_{mk}I_{rk}^{calc} - V_{rk}I_{mk}^{calc}}{V_k^2}. \tag{2.43}$$

Jacobian structure:

The proposed current injection based NR PF equation can be compactly expressed as,

$$
\begin{bmatrix} \Delta I_{rm}^{pq} \\ \Delta I_{rm}^{pv} \end{bmatrix} = \begin{bmatrix} J_{pq-pq} & J_{pq-pv} \\ J_{pv-pq} & J_{pv-pv} \end{bmatrix} \begin{bmatrix} \Delta V_{rm}^{pq} \\ \Delta V_{mQ}^{pv} \end{bmatrix}. \tag{2.44}
$$

Where,

$$
\Delta I_{rm}^{pq} = \begin{bmatrix} \Delta I_{r1}, \Delta I_{r2}, \ldots, \Delta I_{rn}, \Delta I_{m1}, \Delta I_{m2}, \ldots, \Delta I_{mn} \end{bmatrix}^T,
$$

$$
\Delta I_{rm}^{pv} = \begin{bmatrix} \Delta I_{r(n+1)}, \Delta I_{r(n+2)}, \ldots, \Delta I_{rN}, \Delta I_{m(n+1)}, \Delta I_{m(n+2)}, \ldots, \Delta I_{mN} \end{bmatrix}^T,
$$

$$
\Delta V_{rm}^{pq} = \begin{bmatrix} \Delta V_{r1}, \Delta V_{r2}, \ldots, \Delta V_{rn}, \Delta V_{m1}, \Delta V_{m2}, \ldots, \Delta V_{mn} \end{bmatrix}^T,
$$

$$
\Delta V_{mQ}^{pv} = \begin{bmatrix} \Delta V_{m(n+1)}, \Delta V_{m(n+2)}, \ldots, \Delta V_{mN}, \Delta Q_{(n+1)}, \Delta Q_{(n+2)}, \ldots, \Delta Q_N \end{bmatrix}^T,
$$

$$
J_{pq-pq} = \left[\begin{array}{c|c} \mathbf{G}' & \mathbf{B}' \\ \hline \mathbf{B}'' & \mathbf{G}'' \end{array} \right],
$$

$$
J_{pq-pv} = \left[\begin{array}{c|c} -\mathbf{B} - \frac{V_m}{V_r}\mathbf{G} & 0 \\ \hline \mathbf{G} - \frac{V_m}{V_r}\mathbf{B} & 0 \end{array} \right],
$$

$$
J_{pv-pv} = \left[\begin{array}{c|c} \mathbf{B}^{*\prime} - \frac{V_m}{V_r}\mathbf{G}^{*\prime} & -\frac{V_m}{V^2} \\ \hline \mathbf{G}^{*\prime\prime} - \frac{V_m}{V_r}\mathbf{B}^{*\prime\prime} & \frac{V_r}{V^2} \end{array} \right] \text{ and,}
$$

$$
J_{pv-pq} = \left[\begin{array}{c|c} \mathbf{G} & -\mathbf{B} \\ \hline \mathbf{B} & \mathbf{G} \end{array} \right].
$$

The above-described formulation of PF is more accurate for the distribution systems because it gives more accurate modeling of PV buses as compared to model suggested in [57] . Modeling of voltage dependency is incorporated with other models of components.

2.3   Proposed Algorithms

Three different PF algorithms are described in this section. These techniques are based on the system of non-linear equations and ordinary differential equations. This section is divided into three subsections: algorithms based on Conventional NR technique, algorithms based on the LM technique, and algorithms based on the Runge-Kutte technique.

2.3.1 Modified Newton-Raphson Method

Let us assume a nonlinear equation, $f(x) = 0$, where x represents a variable. If x_0 be an initial predicated solution, then $f(x)$ can be extended around x_0 using Taylor series.

$$f(x) = 0, \text{ and } f(x)$$
$$= f(x_0) + f'(x_0)(x - x_0) + \frac{1}{2!}f''(x_0)(x - x_0)^2 + \dots + \frac{1}{n!}f^n(x_0)(x - x_0)^n + \dots, \tag{2.45}$$

where, $f^n(x_0)$ is $n-$th derivative of $f(x)$ at $x = x_0$.

By neglecting the higher order derivatives (second and higher order) of $f(x)$ from Equation 2.45 yields

$$f(x) \simeq f(x_0) + f'(x_0)(x - x_0) = 0 \tag{2.46}$$

From Equation 2.46, x^* can be calculated as follows.

$$x^* = x_0 - \frac{f(x_0)}{f'(x_0)}, \tag{2.47}$$

where x^* is a predicated value of x.

Therefore, at $k-$th iteration, the predicated value of x, x^{k+1}, can be calculated by following equation.

$$x^{k+1} = x^k - \triangle x^k, \tag{2.48}$$

where,

$$\triangle x^k = \frac{f(x^k)}{f'(x^k)} \tag{2.49}$$

Equations 2.48 and 2.49 can be generalized for system of non-linear equations by following Equations.

$$\triangle \mathbf{x}^k = \mathbf{J_x}(\mathbf{x}^k)^{-1}\mathbf{F}(\mathbf{x}^k), \tag{2.50}$$

$$\mathbf{x}^{k+1} = \mathbf{x}^k - \triangle \mathbf{x}^k, \tag{2.51}$$

where $\mathbf{x}^k = [x_1^k, x_2^k, \dots, x_n^k]^t$, $\mathbf{F}(\mathbf{x}^k) = [f_1(\mathbf{x}^k), f_2(\mathbf{x}^k), \dots, f_n(\mathbf{x}^k)]^t$, and $\mathbf{J_x}$ represents the Jacobian matrix at $\mathbf{x}^k$.

The main steps of Newton's method are summarized in Algorithm 1.

In this work, one algorithm, named CINR, based on Algorithm 1 is proposed where the current injection based PF formulation are employed in NR method. In CINR, the Jacobian matrix is calculated by using Equation 2.44. To deal with the ill-conditioning of the system, an optimal multiplier is calculated in each iterations using following equation.

$$m^* \leftarrow \text{minimize}(||\mathbf{F_{x - m \triangle x}}||), \tag{2.52}$$

Algorithm 1: Newton's Method

    Data: $\mathbf{x}^0 \leftarrow$ initial predicated solution

    Result: $\mathbf{x}^*$

  1 $\mathbf{F_x} \leftarrow \mathbf{F}(\mathbf{x}^0)$;

  2 $TolF \leftarrow ||\mathbf{F_x}||$;

  3 $\mathbf{J} \leftarrow \mathbf{J_x}(\mathbf{x}^0)$;

  4 $k \leftarrow 0$;

  5 while $TolF \leq 10^{-06}$ **do**

  6 $\triangle\mathbf{x}^k \leftarrow \mathbf{J}^{-1}\mathbf{F_x}$;

  7 $\mathbf{x}^{k+1} \leftarrow \mathbf{x}^{k+} - \triangle\mathbf{x}^k$;

  8 $\mathbf{F_x} \leftarrow \mathbf{F}(\mathbf{x}^{k+1})$;

  9 $TolF \leftarrow ||\mathbf{F_x}||$;

 10 $\mathbf{J} \leftarrow \mathbf{J_x}(\mathbf{x}^{k+1})$;

 11 $k \leftarrow k + 1$;

 12 end

 13 $\mathbf{x}^* \leftarrow \mathbf{x}^k$

---

where

$$\triangle\mathbf{x}^k = \mathbf{J}^{-1}\mathbf{F_x}. \tag{2.53}$$

Then, the solution is updated using following equation.

$$\mathbf{x}^{k+1} = \mathbf{x}^k - m^*\triangle\mathbf{x}. \tag{2.54}$$

Thus, the above modifications relate to finding the optimal value of step-size, m, such that the mismatch vector $F(x)$ is minimized.

2.3.2   Fourth-order Levenberg-Marquardt Method

The LM algorithm belongs to the class of conventional methods that solves the ill-conditioned system of nonlinear equations. At $k-$th iteration, the solution x^k can be estimated using LM algorithm by following Equations.

$$\triangle\mathbf{x}^k = (\mathbf{J_x}(\mathbf{x}^k)^t\mathbf{J_x}(\mathbf{x}^k) + \lambda_k\mathbf{I})^{-1}\mathbf{F}(\mathbf{x}^k), \tag{2.55}$$

$$\mathbf{x}^{k+1} = \mathbf{x}^k - \triangle\mathbf{x}^k, \tag{2.56}$$

where $\mathbf{I}$ represents identity matrix and λ_k can be calculated by Equation (2.57).

$$\lambda_k = \mu||\mathbf{F}(\mathbf{x}^k)||^\sigma, \tag{2.57}$$

where μ and σ are parameters used in LM. A suitable parameter setting is needed to achieve the convergence.

Bi-quadratic Levenberg-Marquardt

High order LM techniques are proficient in lessening the number of Jacobian calculations with better convergence rate as compared to LM. A bi-quadratic LM is introduced in [120]. The steps of bi-quadratic LM are shown in Algorithm 2. A PF algorithm based on Algorithm 2, named LMPF, is proposed in this chapter.

2.3.3 Modified Runge-Kutta Method

In this section, Runge-Kutta algorithm is briefly described. Formulation of system of non-linear equations problem based on conventional NR is discussed in the following paragraph.

Conventional Newton-Raphson

A set of ordinary differential equations can be presented by following equations.

$$\dot{\mathbf{x}} = \mathbf{f}(\mathbf{x}) \tag{2.58}$$

The following steps are used in explicit Euler method to integrate the Equation 2.58.

$$\triangle\mathbf{x}^k = \triangle t\mathbf{f}(\mathbf{x}^k), \tag{2.59}$$

$$\mathbf{x}^{k+1} = \mathbf{x}^k + \triangle\mathbf{x}^k, \tag{2.60}$$

where $\triangle t$ represents the time step.

An analogy between system of non-linear equations and ordinary differential equations can be easily established using Equations 2.50, 2.51, 2.59, and 2.60 by defining following relation.

$$\mathbf{f}(\mathbf{x}^k) = \mathbf{J}_\mathbf{x}(\mathbf{x}^k)^{-1}\mathbf{F}(\mathbf{x}^k), \text{ at } \triangle t = 1 \tag{2.61}$$

From above relation, it can be established that any numerical technique, used to solve ordinary differential equations, can be applied on the system of non-linear equations [70].

Algorithm 2: Bi-quadratic LM Method

Data: $\mathbf{x}^0 \leftarrow$ initial predicated solution;

Initial parameter for μ and σ

Result: $\mathbf{x}^*$

1   $\mathbf{F_x} \leftarrow \mathbf{F}(\mathbf{x}^0)$;

2   $TolF \leftarrow ||\mathbf{F_x}||$;

3   $\mathbf{J} \leftarrow \mathbf{J_x}(\mathbf{x}^0)$;

4   $k \leftarrow 0$;

5   **while** $TolF \leq 10^{-06}$ **do**

6     $\lambda_k \leftarrow \mu_k ||\mathbf{F_x}||^\sigma$;

7     $\mathbf{d}^k \leftarrow -(\mathbf{J}^t\mathbf{J} + \lambda_k\mathbf{I})^{-1}\mathbf{J}^t\mathbf{F_x}$;

8     $\mathbf{y}^k \leftarrow \mathbf{x}^k + \mathbf{d}^k$;

9     $\mathbf{F_y} \leftarrow \mathbf{F}(\mathbf{y}^k)$;

10     $\mathbf{dd}^k \leftarrow -(\mathbf{J}^t\mathbf{J} + \lambda_k\mathbf{I})^{-1}\mathbf{J}^t\mathbf{F_y}$;

11     $\mathbf{z}^k \leftarrow \mathbf{y}^{k+} + \mathbf{dd}^k$;

12     $\mathbf{F_z} \leftarrow \mathbf{F}(\mathbf{z}^k)$;

13     $\mathbf{ddd}^k \leftarrow -(\mathbf{J}^t\mathbf{J} + \lambda_k\mathbf{I})^{-1}\mathbf{J}^t\mathbf{F_z}$;

14     $Ared^k \leftarrow ||\mathbf{F_x}||^2 - ||\mathbf{F}(\mathbf{x}^k + \mathbf{d}^k + \mathbf{dd}^k + \mathbf{ddd}^k)||^2$;

15     $Pred^k \leftarrow$
     $||\mathbf{F_x}||^2 - ||\mathbf{F_x}|| + \mathbf{J}(\mathbf{d}^k)^2 + ||\mathbf{F_y}||^2 - ||\mathbf{F_y}|| + \mathbf{J}(\mathbf{dd}^k)^2 + ||\mathbf{F_z}||^2 - ||\mathbf{F_z}|| + \mathbf{J}(\mathbf{ddd}^k)^2$;

16     $r^k \leftarrow \frac{Ared^k}{Pred^k}$;

17   **if** $r^k \geq p_0$ **then**

18       $\mathbf{x}^{k+1} \leftarrow \mathbf{x}^k + \mathbf{d}^k + \mathbf{dd}^k + \mathbf{ddd}^k$;

19       $\mathbf{F}_x \leftarrow \mathbf{F}(\mathbf{x}^{k+1})$;

20       $TolF \leftarrow ||\mathbf{F_x}||$;

21       $\mathbf{J} \leftarrow \mathbf{J_x}(\mathbf{x}^{k+1})$;

22   **end**

23     $k \leftarrow k + 1$;

24   **end**

25   $\mathbf{x}^* \leftarrow \mathbf{x}^k$

Fourth-order Runge-Kutta method

In this work, the RK4 algorithm is adopted to solve the PF problem of the ill-conditioned three-phase power system. The main steps of the Runge-Kutta algorithm are depicted in Algorithm 3.

A PF algorithm based on Algorithm 3, named RK4PF, is used here to solve PF problem of ill-conditioned unbalanced distribution systems. In algorithm 3, steps at statement numbers, $20 - 25$, are the modifications in the existing Runge-kutta method towards adjustment of h, the step-size.

2.4 Results and Discussion

In this section of the chapter, the four proposed PF techniques are validated over the small, medium, large and very large test cases.

2.4.1 Test Systems

The following test systems are utilized to demonstrate the performance of proposed algorithms.

- **CASE13 test system**: This system is radial unbalanced type with 9 branches and 12 PQ buses.

- **CASE25 test system**: This system is radial unbalanced type with 24 branches and 24 PQ buses.

- **CASE37 test system**: This system is radial unbalanced type with 34 branches and 34 PQ buses.

- **CASE28 test system**: This system is radial unbalanced type with 27 branches, 24 PQ buses, and 3 PV buses.

- **CASE56 test system**: This system is radial unbalanced type with 55 branches, 49 PQ buses, and 6 PV buses.

- **CASE84 test system**: This system is radial unbalanced type with 83 branches, 74 PQ buses, and 9 PV buses.

Algorithm 3: RK4PF algorithm

Data: $\mathbf{x}^0 \leftarrow$ initial predicated solution; $h \leftarrow 1$

Result: $\mathbf{x}^*$

1   $\mathbf{F_x} \leftarrow \mathbf{F}(\mathbf{x}^0)$;

2   $TolF \leftarrow ||\mathbf{F_x}||$;

3   $\mathbf{J_x} \leftarrow \mathbf{J_x}(\mathbf{x}^0)$;

4   $k \leftarrow 0$;

5   **while** $TolF \leq 10^{-06}$ **do**

6      $\mathbf{k_1}^k \leftarrow -(\mathbf{J_x})^{-1}\mathbf{F_x}$;

7      $\mathbf{y}^k \leftarrow \mathbf{x}^k + \frac{h}{2}\mathbf{k_1}^k$;

8      $\mathbf{F_y} \leftarrow \mathbf{F}(\mathbf{y}^k)$;

9      $\mathbf{k_2}^k \leftarrow -(\mathbf{J_x}(\mathbf{y}^k))^{-1}\mathbf{F_y}$;

10     $\mathbf{z}^k \leftarrow \mathbf{x}^{k+} + \frac{h}{2}\mathbf{k_2}^k$;

11     $\mathbf{F_z} \leftarrow \mathbf{F}(\mathbf{z}^k)$;

12     $\mathbf{k_3}^k \leftarrow -(\mathbf{J_x}(\mathbf{z}^k))^{-1}\mathbf{F_z}$;

13     $\mathbf{u}^k \leftarrow \mathbf{x}^k + h\mathbf{k_3}^k$;

14     $\mathbf{F_u} \leftarrow \mathbf{Fu}^k$;

15     $\mathbf{k_4}^k \leftarrow -(\mathbf{J_x}(\mathbf{u}^k))^{-1}\mathbf{F_u}$;

16     $\mathbf{x}^{k+1} \leftarrow \mathbf{x}^k + \frac{h}{6}(\mathbf{k_1}^k + 2\mathbf{k_2}^k + 2\mathbf{k_3}^k + \mathbf{k_4})$;

17     $\mathbf{F}_x \leftarrow \mathbf{F}(\mathbf{x}^{k+1})$;

18     $TolF \leftarrow ||\mathbf{F_x}||$;

19     $\mathbf{J} \leftarrow \mathbf{J_x}(\mathbf{x}^{k+1})$;

20     $\chi \leftarrow ||\mathbf{k_2}^k - \mathbf{x}^{k+1}||_\infty$;

21   **if** $\chi \geq 001$ **then**

22        $h \leftarrow \max\{0.985h, 0.75\}$;

23   **else**

24        $h \leftarrow \max\{1.015h, 0.75\}$;

25   **end**

26     $k \leftarrow k + 1$;

27 **end**

28 $\mathbf{x}^* \leftarrow \mathbf{x}^k$

- **CASE112 test system**: This system is radial unbalanced type with 111 branches, 99 PQ buses, and 12 PV buses.

- **CASE392 test system**: This system is radial unbalanced type with 391 branches, 349 PQ buses, and 42 PV buses.

- **CASE784 test system**: This system is radial unbalanced type with 783 branches, 699 PQ buses, and 84 PV buses.

- **CASE1176 test system**: This system is radial unbalanced type with 1175 branches, 1049 PQ buses, and 126 PV buses.

The above-mentioned test systems are well-conditioned at normal operating point. Since the performance of algorithms are to be analyzed on ill-conditioned systems, the condition of the test systems are deteriorated by increasing the loading levels at the PQ buses and r/x ratios of the branches. In addition, the flat initial start is applied in each algorithm to solve the PF problem of these test cases. The details of the above test cases and their modification are described in Appendix-I.

2.4.2 Parameter Settings of Algorithms

In this work, three robust PF techniques, named CINR, LMPF, and RK4PF, are proposed to solve the PF problem of ill-conditioned distribution test systems. The following parameter setting is adopted in the algorithms.

- **CINR**: $TolF = 10^{-06}$, $m0 = 1$, and $Max\_iter = 100$.

- **LMPF**: $TolF = 10^{-06}$, $\mu = 1.3$, $\sigma = 1$, $\rho_0 = 0.5$, and $Max\_iter = 100$.

- **RK4PF**: $TolF = 10^{-06}$, $h = 1$, and $Max\_iter = 300$.

All algorithms have been tested out on PC Intel Core i7-7700 3.60 GHz using MAT-LAB R2017b.

2.4.3 Validation of Proposed Algorithms

In this section, the accuracy of the proposed algorithms are validated on ill-conditioned version of CASE13 and CASE28 test systems. These test systems cannot be solved by

using conventional algorithms, TCIM, iTCIM, and BFS due to their ill-conditioning. Very few works based on the Newton-Raphson algorithm have been done on power flow problem of ill-conditioned distribution systems. The backward-forward sweep algorithm is a popular algorithm for the distribution system, but this algorithm do not converge on true solution of the power flow problem. Hence, there is no solution obtained which can be compared with our converged solution. Therefore, candidate could not validate the result of proposed algorithms with the result of other algorithms from the literature. However, the power flow problem of power system is a type of system of non-linear equations, where power flow equations are treated as system and solution of this system is power flow solution. As far as validation of power flow methods are concerned, they get validated when the solution of non-linear equations get solved accurately.

The precise idea behind taking the scenario of heavily loaded and ill-conditioned system was to investigate whether the proposed method can handle such scenarios. It is obvious that in the said scenarios, the system may have low system voltages. The load flow is planning tool which computes system voltages under full spectrum of loading to plan the operational strategies. A similar approach for investigating the unbalanced load scenario was also adopted. The severe system situations were deliberately adopted to show the enhanced capability of the proposed methods and approaches in terms of convergence and accuracy.

CASE13 test system

The structure of this test system is similar to the standard CASE13 test system. The PF solution of this test system is worked out using proposed algorithms and is depicted in Tables 2.1, 2.2, and 2.3. From these Tables, it can be concluded that the PF solution obtained from all the solutions is similar to each other with minor variations. Note that the optimal values of the step-size in case of CINR are calculated as 0.9811, 1.2457, and 0.5734. The system used here is an unbalanced test system. When we increase the loads on all buses such that the system operates in an ill-conditioned zone, the loads will be more unbalanced in the system. Therefore, in this case voltages are expected to be low at buses 7, 8, 9, and 10 in respective phases. Nose curve of case13 has been drawn in Figure 2.1. From Figure 2.1, it is verified that the obtained voltages for the given loading condition are quite low as expected. However, they are not intended as operational voltages for a
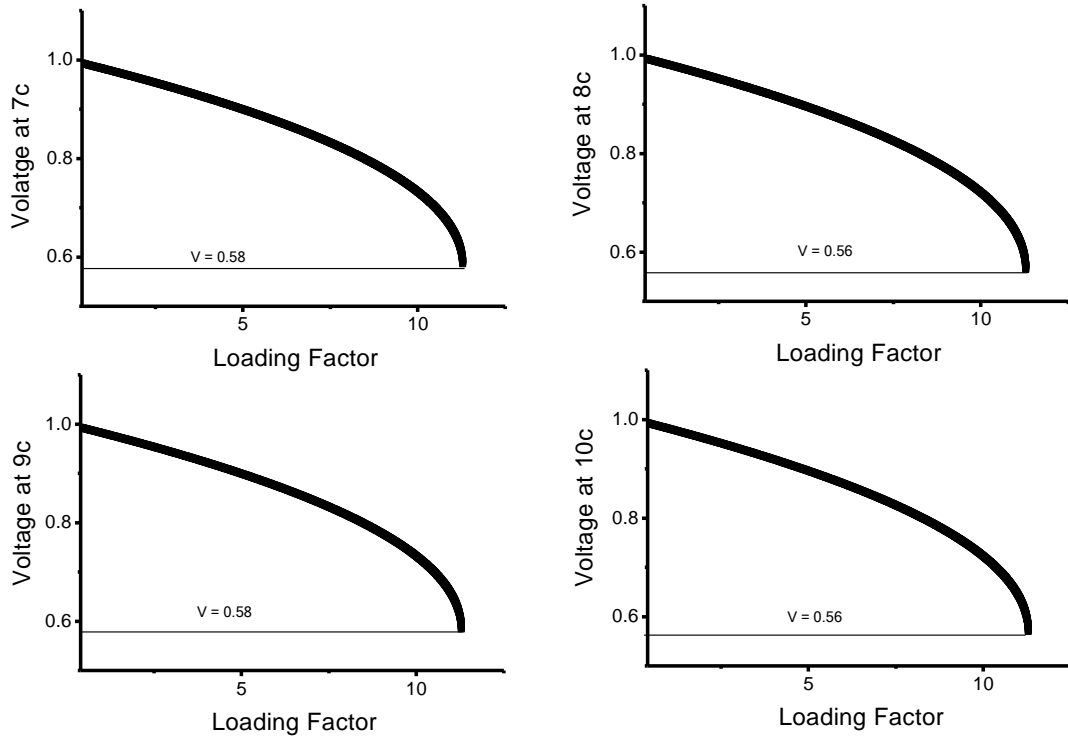
Figure 2.1: Nose curve (PV curve) of bus 7c, 8c, 9c, and 10c.

system. These are in fact the solutions obtained in planning scenario.

Table 2.1: PF solution of ill-conditioned version of CASE13 system using CINR

	CINR					
Bus No.	$|V_a|$	$\angle_a$	$|V_b|$	$\angle_b$	$|V_c|$	$\angle_c$
1	1.00	0.00	1.00	-120.00	1.00	120.00
2	0.99	-0.22	0.99	-120.16	0.99	119.98
3	–	–	–	–	0.55	99.10
4	–	–	0.95	-120.65	1.01	119.63
5	–	–	0.93	-120.94	1.02	119.52
6	0.96	-13.42	–	–	–	–
7	0.98	-13.57	1.04	-117.21	0.58	101.56
8	0.97	-14.67	1.05	-117.44	0.56	101.05
9	0.98	-13.57	1.04	-117.21	0.58	101.56
10	0.98	-13.69	–	–	0.57	100.49

The convergence characteristics of all proposed algorithms on CASE13 ill-conditioned test system are depicted in Figure 2.2. From this figure, it can be concluded that the convergence characteristics of the proposed algorithm are different from each other. In the case of CINR, the convergence rate is faster than the other algorithms. RK4PF

Table 2.2: PF solution of ill-conditioned version of CASE13 test system using LMPF

	LMPF					
Bus No.	$|V_a|$	$\angle_a$	$|V_b|$	$\angle_b$	$|V_c|$	$\angle_c$
1	1.00	0.00	1.00	-120.00	1.00	120.00
2	0.99	-0.22	0.99	-120.16	0.99	119.98
3	–	–	–	–	0.55	99.10
4	–	–	0.95	-120.65	1.01	119.63
5	–	–	0.93	-120.94	1.02	119.52
6	0.96	-13.43	–	–	–	–
7	0.98	-13.59	1.04	-117.24	0.58	101.56
8	0.96	-14.70	1.05	-117.47	0.56	101.04
9	0.98	-13.58	1.04	-117.26	0.58	101.58
10	0.98	-13.70	–	–	0.57	100.49

Table 2.3: PF solution of ill-conditioned version of CASE13 system using RK4PF

	RK4PF					
Bus No.	$|V_a|$	$\angle_a$	$|V_b|$	$\angle_b$	$|V_c|$	$\angle_c$
1	1.00	0.00	1.00	-120.00	1.00	120.00
2	0.99	-0.22	0.99	-120.16	0.99	119.98
3	–	–	–	–	0.55	99.10
4	–	–	0.95	-120.65	1.01	119.63
5	–	–	0.93	-120.93	1.02	119.52
6	0.96	-13.47	–	–	–	–
7	0.99	-13.61	1.04	-117.13	0.58	101.55
8	0.97	-14.72	1.05	-117.36	0.56	101.05
9	0.99	-13.61	1.04	-117.13	0.58	101.55
10	0.98	-13.74	–	–	0.56	100.49

algorithm has a low convergence rate. Furthermore, the value of tolerance is least in the case of LMPF.

The above discussion concludes that the all the proposed algorithms are robust PF tool for ill-conditioned unbalanced test systems. CINR is a faster algorithm than others and LMPF has provided most accurate PF solution than other algorithms.

CASE28 test system

To explore the acceptance of the proposed algorithms for multi-source three-phase unbalanced radial networks, proposed algorithms are tested on an ill-conditioned CASE28 test system.

CASE28 represents an ill-conditioned unbalanced distribution system which includes 28-buses with four power sources (1-slack and 3-PV bus). This system can serve
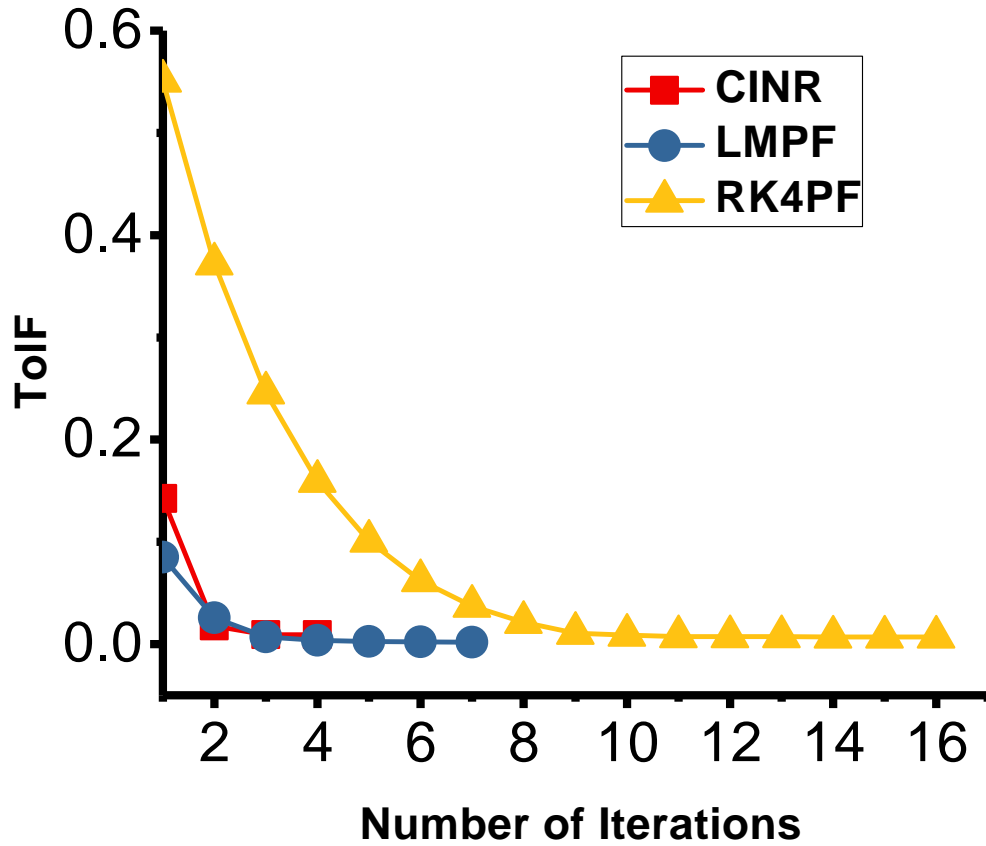
Figure 2.2: Convergence characteristics of CASE13(ill-conditioned case) using CINR, LMPF, and RK4PF.

as a benchmark test system to investigate the robustness of the algorithm over the ill-conditioned system because conventional methods fail to converge on the PF solution.

PF solution obtained from all proposed algorithms are reported in Tables 2.4, 2.5, and 2.6. These tables show that all the algorithms provide a similar solution with minor variations because all the algorithm stop solving at different accuracy level after fulfilling the specified tolerance.

To show the convergence characteristics of these algorithms, convergence curve of these algorithms is depicted in Figure 2.3. On the contrary to accuracy, the convergence characteristics of these algorithms are different from each other. CINR has the fastest convergence speed among all algorithms, but initially the convergence is slower than LMPF and RK4PF because of linear convergence rate. RK4PF has shown the least convergence speed among all of them. LMPF has provided the most accurate results with moderate convergence speed.

Table 2.4: PF solution of ill-conditioned version of CASE28 test system using CINR

	CINR					
Bus No.	$|V_a|$	$\angle_a$	$|V_b|$	$\angle_b$	$|V_c|$	$\angle_c$
1	1.00	0.00	1.00	-120.00	1.00	120.00
2	0.93	-15.53	0.95	-129.59	0.97	111.49
3	0.93	-18.67	0.95	-131.78	0.97	109.68
4	0.94	-20.22	0.95	-132.86	0.97	108.84
5	0.93	-20.21	0.95	-132.84	0.96	108.83
6	0.85	-24.03	0.90	-134.42	0.92	106.97
7	0.81	-33.81	0.87	-139.71	0.89	102.09
8	0.84	-24.01	0.89	-134.39	0.91	106.96
9	0.77	-33.82	0.83	-139.67	0.86	102.05
10	0.73	-33.82	0.80	-139.65	0.84	102.02
11	0.72	-33.83	0.79	-139.65	0.83	102.02
12	0.71	-33.82	0.78	-139.64	0.82	102.05
13	0.71	-33.82	0.78	-139.65	0.82	102.03
14	0.84	-43.69	0.89	-145.10	0.91	97.17
15	0.83	-43.67	0.88	-145.09	0.90	97.16
16	0.80	-33.80	0.86	-139.70	0.89	102.08
17	0.83	-43.67	0.89	-145.09	0.90	97.18
18	0.93	-21.38	0.94	-133.78	0.95	108.03
19	0.93	-24.05	0.94	-135.82	0.95	106.47
20	0.94	-24.08	0.95	-135.83	0.96	106.41
21	0.91	-21.34	0.92	-133.74	0.93	108.10
22	0.90	-21.32	0.91	-133.71	0.92	108.15
23	0.92	-20.21	0.94	-132.86	0.95	108.81
24	0.91	-20.21	0.93	-132.88	0.94	108.80
25	0.89	-20.17	0.92	-132.93	0.93	108.82
26	0.99	-22.47	0.99	-134.24	0.99	107.98
27	0.98	-50.96	0.98	-148.59	0.99	94.21
28	0.99	-26.17	0.99	-137.27	0.99	105.46

2.4.4 Comparison of Algorithms

The proposed algorithms are compared with the following standard PF technique of distribution systems:

- TCIM [24]: NR-based three phase PF algorithm using current injection equations.

- iTCIM [57]: A second order NR-based three phase PF algorithm using current injection equations.

- BFS [121]: A three phase PF algorithm based on backward/forward sweep algorithm.

Table 2.5: PF solution of ill-conditioned version of CASE28 test system using LMPF

	LMPF					
Bus No.	$|V_a|$	$\angle_a$	$|V_b|$	$\angle_b$	$|V_c|$	$\angle_c$
1	1.00	0.00	1.00	-120.00	1.00	120.00
2	0.93	-15.64	0.95	-129.67	0.97	111.33
3	0.93	-18.83	0.95	-131.88	0.97	109.49
4	0.94	-20.40	0.95	-132.98	0.97	108.64
5	0.93	-20.39	0.95	-132.96	0.96	108.63
6	0.85	-24.18	0.90	-134.52	0.92	106.72
7	0.81	-34.02	0.87	-139.84	0.89	101.73
8	0.83	-24.16	0.89	-134.49	0.91	106.71
9	0.76	-33.99	0.83	-139.78	0.86	101.69
10	0.73	-33.97	0.80	-139.75	0.83	101.65
11	0.72	-33.96	0.79	-139.74	0.82	101.65
12	0.71	-33.95	0.78	-139.72	0.82	101.69
13	0.71	-33.95	0.78	-139.73	0.82	101.67
14	0.84	-44.04	0.89	-145.30	0.91	96.71
15	0.82	-44.01	0.88	-145.29	0.90	96.69
16	0.80	-34.01	0.86	-139.83	0.89	101.73
17	0.83	-44.01	0.88	-145.29	0.90	96.72
18	0.93	-21.58	0.94	-133.91	0.95	107.82
19	0.93	-24.28	0.94	-135.99	0.95	106.23
20	0.94	-24.32	0.95	-135.99	0.96	106.17
21	0.91	-21.53	0.92	-133.87	0.93	107.88
22	0.89	-21.51	0.91	-133.84	0.92	107.93
23	0.92	-20.39	0.94	-132.98	0.95	108.61
24	0.91	-20.38	0.93	-133.00	0.94	108.60
25	0.89	-20.35	0.92	-133.05	0.93	108.62
26	0.99	-22.67	0.99	-134.41	0.99	107.78
27	0.98	-51.22	0.98	-148.94	0.99	93.93
28	0.99	-26.42	0.99	-137.49	0.99	105.23

The above-mentioned algorithms have been implemented on MATLAB environment to perform the experiments.

Well-conditioned Systems

The PF analysis of well-conditioned test systems is performed by applying proposed algorithms and other popular conventional techniques: TCIM, iTCIM, and BFS. For this investigation, the following test systems are considered: CASE13, CASE25, CASE37, CASE28, CASE56, CASE84, CASE112, CASE140, CASE168, and CASE196. The system data of these test systems is available at `https://github.com/abhisheka456`.

The total number of iterations of all algorithms for converging on all these test

Table 2.6: PF solution of ill-conditioned version of CASE28 test system using RK4PF

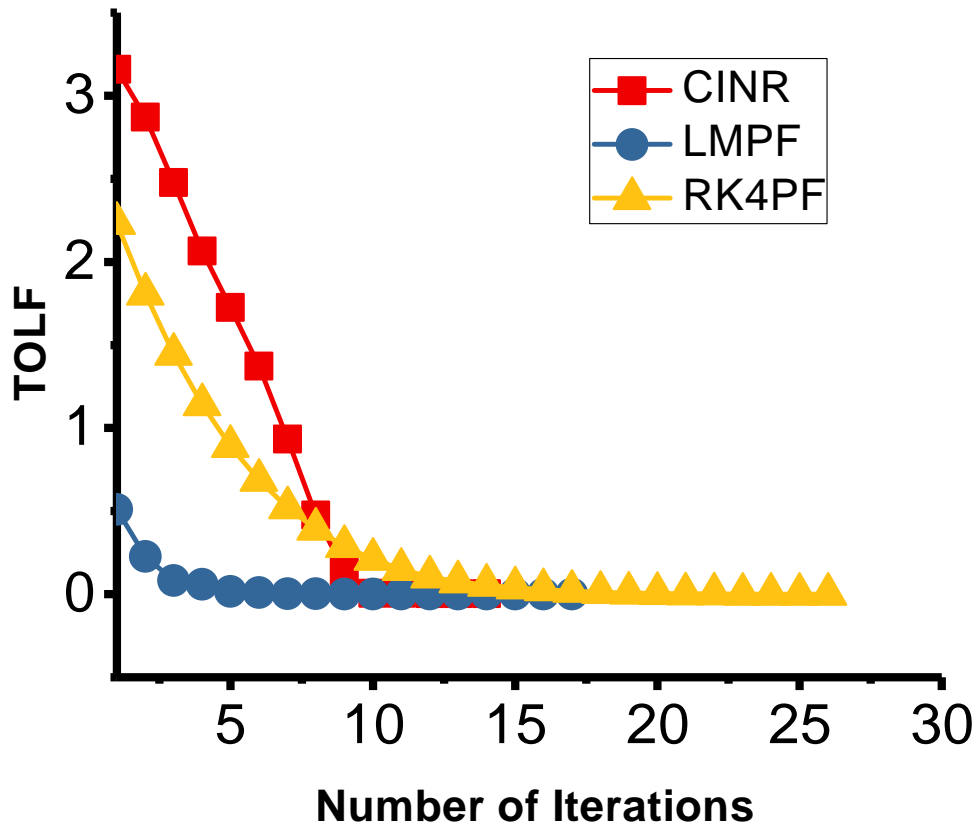|	RK4PF					
Bus No.	$|V_a|$	$\angle_a$	$|V_b|$	$\angle_b$	$|V_c|$	$\angle_c$
1	1.00	0.00	1.00	-120.00	1.00	120.00
2	0.93	-15.57	0.95	-129.68	0.97	111.40
3	0.93	-18.73	0.95	-131.88	0.97	109.58
4	0.94	-20.30	0.95	-132.97	0.97	108.74
5	0.93	-20.29	0.95	-132.96	0.96	108.73
6	0.85	-24.07	0.90	-134.55	0.92	106.81
7	0.81	-33.88	0.87	-139.90	0.89	101.84
8	0.84	-24.05	0.89	-134.53	0.91	106.80
9	0.76	-33.87	0.83	-139.86	0.86	101.81
10	0.73	-33.86	0.80	-139.84	0.84	101.78
11	0.72	-33.86	0.79	-139.84	0.82	101.78
12	0.71	-33.84	0.78	-139.82	0.82	101.82
13	0.71	-33.84	0.78	-139.84	0.82	101.80
14	0.84	-43.83	0.89	-145.35	0.91	96.83
15	0.82	-43.81	0.88	-145.34	0.90	96.82
16	0.80	-33.87	0.86	-139.89	0.89	101.84
17	0.83	-43.81	0.88	-145.35	0.90	96.85
18	0.93	-21.46	0.94	-133.90	0.95	107.93
19	0.93	-24.15	0.94	-135.96	0.95	106.35
20	0.94	-24.19	0.95	-135.97	0.96	106.29
21	0.91	-21.42	0.92	-133.86	0.93	107.99
22	0.89	-21.40	0.91	-133.83	0.92	108.04
23	0.92	-20.29	0.94	-132.97	0.95	108.71
24	0.91	-20.28	0.93	-132.99	0.94	108.70
25	0.89	-20.24	0.92	-133.04	0.93	108.72
26	0.99	-22.56	0.99	-134.39	0.99	107.89
27	0.98	-50.97	0.98	-148.94	0.99	94.05
28	0.99	-26.28	0.99	-137.45	0.99	105.37

Figure 2.3: Convergence characteristics of CASE28 (ill-conditioned case) using CINR, LMPF, and RK4PF.

systems are illustrated in Table 2.7. It can be observed from Table 2.7 that the proposed algorithm NICR and LMPF have presented the fastest convergence rate among all the methods considered, in all the test cases and RK4PF has yielded the least convergence rate. BFS does not converge on multi-source test cases.

The performance of the proposed algorithms is further examined on multi-source large test systems: CASE392, CASE784, and CASE1176. The system data of these test systems is available at `https://github.com/abhisheka456`. The obtained outcomes are presented in Table 2.8. From Table 2.8, it can be observed that the proposed algorithms are more robust than other algorithms on large test systems. In addition, CINR and LMP exhibit the fastest convergence speed among all algorithms while RK4PF shows the least convergence speed. Moreover, the execution time consumed by all algorithms is also calculated and reported in Table 2.9. From Table 2.9, CINR is the most efficient algorithm while RK4PF is consuming more time than the other algorithms. However, the

robustness of RK4PF is better than the other algorithms.

From the above evaluation, it can be concluded that the proposed algorithms, CINR and LMPF are the fastest algorithms among all the methods considered, on well-conditioned test systems. However, the RK4PF demands a large number of iterations for convergence.

Table 2.7: Obtained results of CINR, LMPF, RK4PF, BFS, TCIM, and iTCIM over several test systems. (NC: Not Converged)

Test System	CINR	LMPF	RK4PF	BFS	TCIM	iTCIM
CASE13	2	2	17	6	3	3
CASE25	1	2	15	7	3	3
CASE37	1	2	15	9	2	2
CASE28	2	2	25	NC	3	3
CASE56	3	2	26	NC	6	4
CASE84	3	2	26	NC	6	4
CASE112	3	3	26	NC	6	4
CASE140	3	3	26	NC	6	4
CASE168	3	3	26	NC	7	4
CASE196	3	3	26	NC	7	4

Table 2.8: Obtained results of CINR, LMPF, RK4PF, BFS, TCIM, and iTCIM over large test systems. (NC: Not Converged)

Test System	CINR	LMPF	RK4PF	BFS	TCIM	iTCIM
CASE392	4	4	30	NC	19	5
CASE784	5	5	30	NC	NC	5
CASE1176	5	5	30	NC	NC	5

Table 2.9: Execuation time (in sec) of CINR, LMPF, RK4PF, BFS, TCIM, and iTCIM. (NC: Not Converged)

Test System	CINR	LMPF	RK4PF	BFS	TCIM	iTCIM
CASE13	0.0628	0.1790	0.3313	0.1032	0.0815	0.1048
CASE25	0.0997	0.2691	0.4235	0.1882	0.1206	0.1483
CASE37	0.1392	0.3530	0.4509	0.2610	0.2021	0.2615

Ill-conditioned systems

In section 2.4.3, two ill-conditioned test systems were already utilized to validate the robustness and accuracy of the proposed algorithms. Furthermore, the proposed algorithms

are evaluated on the test systems with high loading conditions and a high r/x ratio. These conditions make the PF equations of the test systems ill-conditioned. Conventional NR algorithms and conventional techniques may diverge on test systems with these conditions or take large number of iterations to converge.

Table 2.10: Total Number of iterations required for different PF algorithms in heavily loaded ill-conditioned systems.(LF: Loading Factor, NC: Not Converged)

CASE37						
LF(%)	CINR	LMPF	RK4PF	BFS	TCIM	iTCIM
200	2	3	16	6	3	3
600	2	3	17	7	3	3
1000	2	3	18	8	3	3
1400	3	4	18	9	4	4
1800	4	21	59	NC	NC	NC
2200	4	24	87	NC	NC	NC
2400	NC	26	88	NC	NC	NC
2500	NC	37	91	NC	NC	NC

CASE84						
LF(%)	CINR	LMPF	RK4PF	BFS	TCIM	iTCIM
100	3	2	26	NC	6	4
200	4	4	28	NC	13	7
300	6	5	29	NC	20	9
400	9	6	29	NC	33	11
500	17	9	29	NC	69	15
600	NC	40	43	NC	NC	NC
700	99	38	63	NC	NC	NC
800	31	35	87	NC	NC	NC

Test systems with high loading conditions

In this section, the stability of proposed algorithms is evaluated on various test systems with different loading conditions. The loading level at the buses of the different test systems is gradually increased to their maximum loading limit. Two test systems, CASE37 and CASE84, are considered for this analysis. Total number of iterations required by different algorithms for CASE37 and CASE84 are reported in Table 2.10.

It is observed from this table that the performance of proposed algorithms is better than the other conventional algorithms. In CASE37, CINR is the most robust algorithm among the other algorithms while LMPF is more efficient in CASE84. However, the RK4PF algorithm requires a high number of iterations to converge but the robustness of this algorithm is better than CINR.

Table 2.11: Total Number of iterations required for different PF algorithms in ill-conditioned systems with high r/x ratios.(NC: Not Converged)

CASE37						
r/x	CINR	LMPF	RK4PF	BFS	TCIM	iTCIM
2	2	3	15	6	3	3
6	2	4	15	7	3	3
10	2	5	15	8	3	3
14	3	6	15	9	4	4
18	3	18	50	NC	NC	NC
22	3	29	77	NC	NC	NC
24	4	22	78	NC	NC	NC
25	8	38	77	NC	NC	NC

CASE84						
r/x	CINR	LMPF	RK4PF	BFS	TCIM	iTCIM
1	3	2	26	NC	6	4
4	4	4	28	NC	14	6
7	5	5	27	NC	26	8
10	6	7	27	NC	48	10
13	16	16	27	NC	NC	20
14	21	43	59	NC	NC	NC
15	21	57	87	NC	NC	NC
16	21	39	94	NC	NC	NC

Test systems with high r/x ratio

The sensitivity of proposed algorithms is validated over different r/x ratios of the lines of test systems and the performance of proposed algorithms is compared with other algorithms. In this study, CASE37 and CASE84 are considered with different r/x ratios.

Number of iterations required to converge by the proposed algorithms with other algorithms are reported in Table 2.11. It can be observed that the proposed algorithms outperform the other conventional algorithms. CINR and LMPF are more efficient than RK4PF and other conventional algorithms.

2.5 Summary

In this chapter, the PF problem of the well and the ill-conditioned unbalanced distribution systems have been solved using the proposed algorithms. Three algorithms using different strategies are proposed. The first algorithm, CINR, is based on conventional NR method with optimal calculation of step-size, m. Other two algorithm, LMPF and RK4PF, consider PF problem as least-square optimization problem and ordinary differential equations problem, respectively. The step-size of these algorithms are adapted to improve their efficiency and robustness. These proposed algorithms are robust and efficient as compared to conventional PF algorithms. The proposed algorithms have been validated over several small, medium and large ill-conditioned unbalanced distribution test systems. The obtained outcomes reveal the superiority and effectiveness of the proposed PF methodology as compared to conventional techniques.

The maximum loadability limit of an unbalanced distribution system is also required to study the power system stability. Proposed algorithms can also be utilized to find the maximum loadability limit. However, the robustness of the algorithms is deteriorated as the system reaches the maximum loadability. In order to address these issues, the application of evolutionary algorithms is analyzeds in the next chapter.